Perforation of welded aluminum extrusions

Numerical prediction and experimental validation

Jens Kristian Holmen[1,a], Tore Børvik[1], Ole Runar Myhr[1,2], and Odd Sture Hopperstad[1]

[1] Structural Impact Laboratory (SIMLab), Department of Structural Engineering, Norwegian University of Science and Technology, NO-7491 Trondheim, Norway

[2] Hydro Aluminium, Research and Technology Development (RTD), NO-6601 Sunndalsora, Norway

Abstract. A purely numerical procedure for predicting the perforation resistance of welded extruded AA6082-T6 aluminum profiles is presented in this study. The numerical work was conducted completely independent of the experimental tests that were only used for validation purposes. The outline of the three-step numerical procedure is as follows: (1) the temperature development due to a specified welding process is predicted by a thermal solver, (2) based on the chemical composition of the alloy, the temperature-time history during aging and the welding analysis, the yield strength and flow stress of the material were determined; and (3) the ballistic limit velocity is found using explicit finite element simulations. The experimental validation program is described and it shows that the ballistic limit velocities found from the impact experiments correlate closely with the numerically predicted values obtained without any physical material or component tests. Further, welding of the 10 mm thick extrusions gives a 10% degradation of the capacity in terms of ballistic limit velocity compared to the unaffected material.

1. Introduction

Johnsen et al. [1] showed that from knowing only the chemical composition of an AA6xxx aluminum alloy and the thermal history during aging we can predict how rolled plates behave under impact loading without conducting any experiments whatsoever. However, real structural parts are commonly connected by bolts, nuts, or weldments, and connections are in many cases weaker than the rest of the structure and require special attention. Welding generates a relatively weak zone compared to the base material, known as the heat affected zone (HAZ). Under normal circumstances ballistic performance is governed by material strength [2,3], so welding may significantly decrease the capabilities of aluminum extrusions to withstand impacts by small-arms bullets.

This study describes the numerical procedure employed to predict the ballistic behavior of welded, flat extruded aluminum profiles of 10 mm thickness. Figure 1 illustrates the three-step procedure where the chemical composition of the material, the artificial aging history of the extrusion, and the welding procedure of the final specimen are used to determine the spatial distribution of yield strength and the flow stress which in turn serves as input to solve the impact problem. Experimental data has only been used to validate the numerical results in this study.

2. Numerical procedure

2.1. Welding simulation

How the temperature evolves through the welding process is predicted by the thermal solver WELDSIM [4]. Welding of the 10 mm thick plates in this study requires three weld-passes. The result is a complex thermal situation in the heat affected zone which is accounted for in the simulations. Symmetry along the welding line was assumed; an arc efficiency of 0.8 was applied and the same values for current, voltage and welding speed as in the experimental program in Sect. 3 were used. The temperature-time history found from the WELDSIM simulation was used as input in the subsequent work.

2.2. Strength evaluation

Evaluation of the strength evolution was done in the nano-scale material model NaMo [6]. This tool predicts the microstructural changes taking place during artificial aging, welding, and room temperature storing. NaMo consists of three separate modules. The first module determines the particle size distribution and the solute content. Using these data and relations from dislocation mechanics, the two last modules calculate the yield strength and the work hardening of the alloy, respectively. A brief description of the model can be found in Ref. [7].

NaMo-analyses of the base material and the material at locations $x = 4.1$ mm, 6.1 mm, 8.1 mm, 10.1 mm and 14.1 mm away from the weld center line were conducted. The output from the analyses were the equivalent stress-equivalent plastic strain curves shown in Fig. 2. NaMo predicts that the base material is the strongest, while the

[a] Corresponding author: jens.k.holmen@ntnu.no
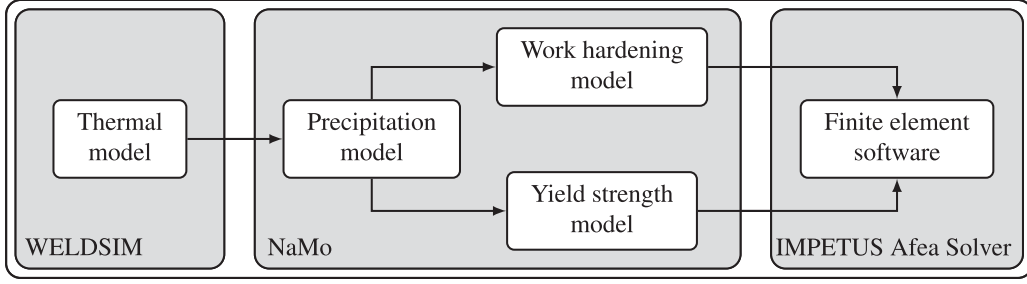
Figure 1. Systematic illustration of the various tools used to predict the ballistic behavior of the aluminum extrusions in this study. Adapted from Ref. [5].
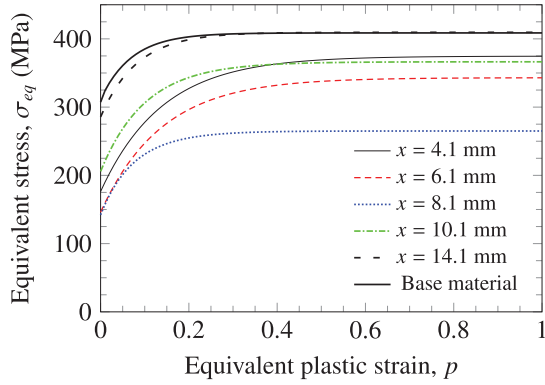
Figure 2. The resulting flow-stress curves obtained from NaMo. These curves determine the hardening behavior used in IMPETUS Afea Solver. Here x is defined as the distance from the weld center line.

weakest part of the HAZ is predicted to be 8.1 mm away from the weld center line.

2.3. Finite element simulations

IMPETUS Afea Solver [8], an explicit finite element solver, was used to simulate the impact process. A thermoelastic-thermoviscoplastic constitutive model [9] based on the well-known Johnson-Cook flow-stress relation [10] was implemented:

$$\sigma_{eq} = \left(\sigma_0 + R(p)\right)\left(1 + \frac{\dot{p}}{\dot{p}_0}\right)^c \left(1 - T^{*m}\right)$$
$$R(p) = \sum_{i=1}^{2} Q_i \left(1 - \exp(-C_i p)\right) \tag{1}$$

where p is the equivalent plastic strain, σ_0 is the quasi-static yield strength and Q_1, C_1, Q_2, C_2 are hardening parameters in the extended Voce work hardening rule. The increased strength due to elevated strain rate $\dot{p}$ is controlled by the strain rate parameter c and $\dot{p}_0$ where the latter is a user defined reference strain rate. $T^* = (T - T_r)/(T_m - T_r)$ is the homologous temperature which is a function of the temperature T, the ambient temperature T_r, and the melting temperature of the material T_m. The superscript m is a material parameter controlling strength degradation due to rising temperature. No failure criterion can be

calibrated based on the available numerically obtained data, so a tiny pinhole was introduced through the plate at the point of impact as seen in Fig. 3. Only the hard steel-core part of the entire AP bullet was modeled, partly because the core is rigid relative to the target plate, thus we do not have to rely on additional material data, and partly because it is numerically much easier. It has been shown experimentally that the effect of omitting the brass jacket is limited [11]. Symmetry was employed to save computational time, i.e., a 30° slice of the extrusion was modeled with appropriate symmetry conditions. High-velocity impact is known to be a localized process, so we did not model the whole target plate. This is not expected to affect the simulation results.

The extended Voce hardening rule in Eq. (1) was adapted to the results in Fig. 2, and simulations such as the one shown in Fig. 3 were run with the obtained material parameters found from curve fitting to Fig. 2. The parameters are given in Ref. [7]. Note that each simulation included only one set of material parameters, i.e., no variation of strength was present within a single simulation in this study. The initial-residual velocity pairs are plotted as markers in Fig. 4 where the solid lines follow the Recht-Ipson model for rigid sharp projectiles [12]

$$v_r = \left(v_i^2 - v_{bl}^2\right)^{1/2}. \tag{2}$$

We see that the ballistic limit velocity v_{bl} is the only unknown parameter in Eq. (2). Figure 2 and Fig. 4b suggest that the ballistic limit velocity increases with increasing material strength, as expected.

3. Experimental validation

3.1. Material processing

The AA6082-T6 specimens used in this study were provided by Hydro Aluminium as 0.2 m wide and 2.0 m long extrusions. The main alloying elements are shown in Table 1. To obtain the desired strength of the material the specimens were heated to 175°C for 5 h and 30 min after extrusion.

Automatic MIG-welding was carried out by Marin Aluminium AS. A Safra 5182 welding wire was used as the welding consumable. Measures were taken to ensure that the temperature in the HAZ was lower than 100°C before

$t = 10.5~\mu s$ $t = 24.5~\mu s$ $t = 42.0~\mu s$ $t = 66.5~\mu s$
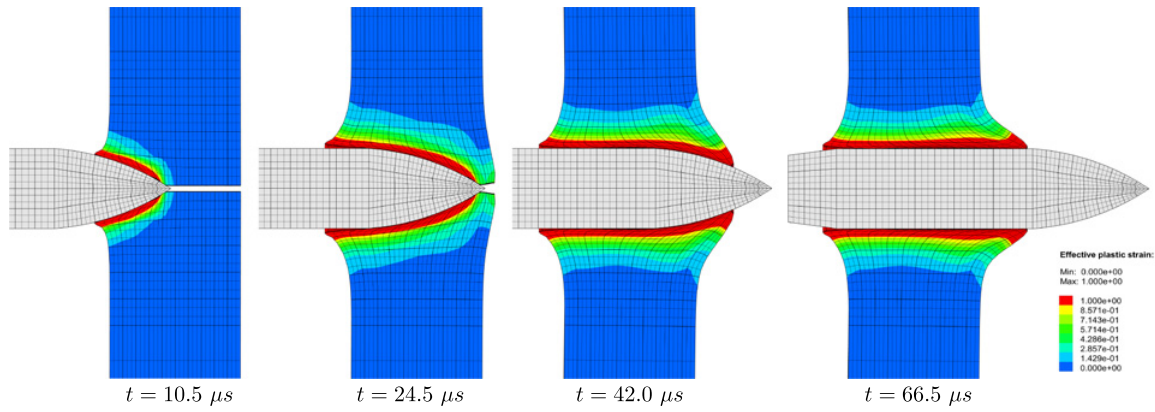
Figure 3. Image series from a typical simulation. The colors show accumulated plastic strain in the range $p \in [0; 1]$, and the mesh is reflected about the centerline to illustrate the pinhole ($v_i = 450.0$ m/s, $v_r = 290.0$ m/s).

(a) Base material

(b) HAZ
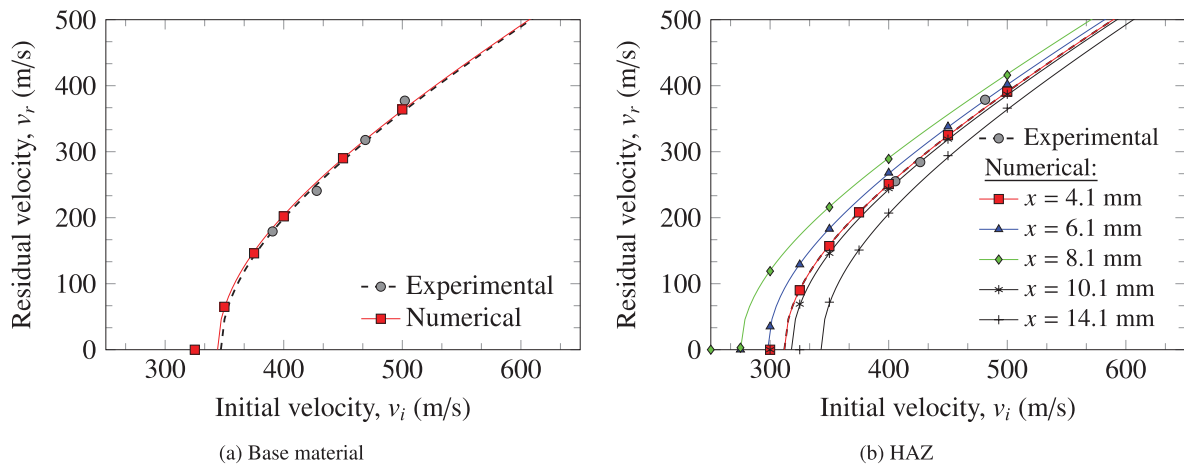
Figure 4. Experimentally determined ballistic limit curves compared to their numerical counterparts for (a) the base material and (b) the HAZ. Here x is defined as the distance from the weld center line.

Table 1. Chemical compostition of the 10 mm thick extrusions of AA6082 aluminum alloy.

Si	Mg	Mn	Fe	Ti	Zn	Cu	Cr	Al
0.93	0.60	0.55	0.18	0.011	0.002	0.008	0.011	Balance

the next weld seam was initiated, this was checked by thermocouples that measured the temperature throughout the welding process.

3.2. Material testing

Three uniaxial tension tests were performed in two directions at $0°$ and $90°$ with respect to the extrusion direction. A laser-scan micrometer measured the diameter reduction in two perpendicular directions all the way to specimen failure while the force was measured by a calibrated load cell in a Zwick/Roell 30 kN testing machine. No significant difference in yield strength, flow stress or failure strain was seen between the tests in the $0°$ and $90°$-directions. A typical result is shown in Fig. 5 where the force F is plotted against the averaged diameter reduction of a specimen taken from the extrusion direction.
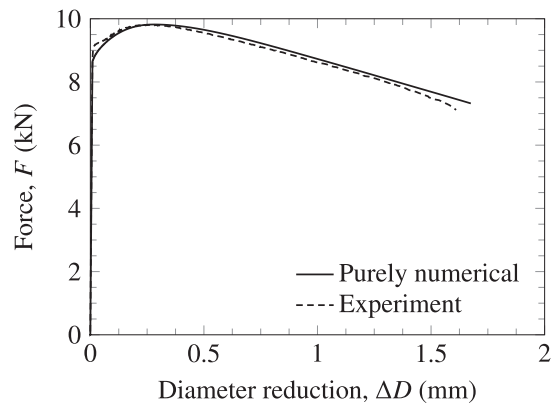
Figure 5. Force-diameter reduction curve for the $0°$-direction from the experiment compared to a simulation based on NaMo results.

Figure 5 also shows that a simulation of the tension test using only numerically obtained data behaves similarly to the experimental result, suggesting that NaMo predicts accurate material behavior for the base material.
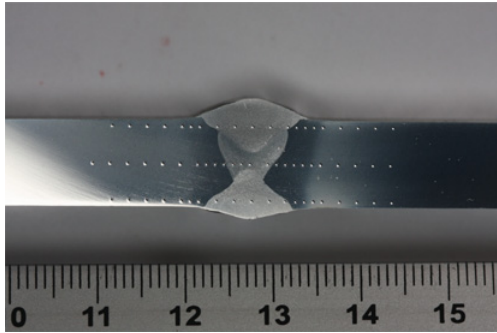
Figure 6. Cross section of the weld. The dots are indentations made by the hardness-test machine.
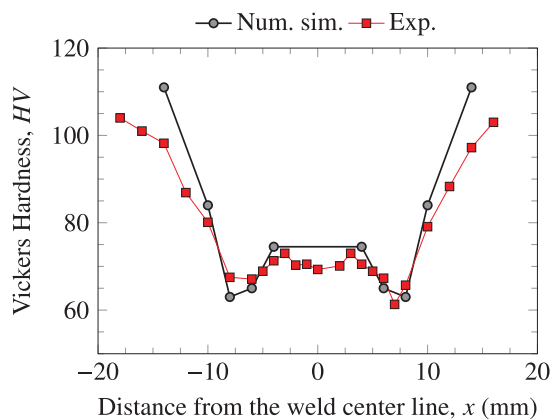
Figure 7. Vickers hardness values obtained from NaMo compared to the hardness measurements.

Hardness tests were performed, and the indented surface is shown in Fig. 6. This was done to get some form of validation of the material behavior in the HAZ. To this end, we applied the following conversion from yield strength (in MPa) to hardness (in VPN) [13]:

$$HV = 0.33\sigma_0 + 16.0 \qquad (3)$$

where HV is the Vickers hardness and σ_0 is the initial yield strength found from Fig. 2. Figure 7 compares the hardness profile through the HAZ at the center of the extrusion (as seen in Fig. 6) to the numerically obtained hardness profile. The numerical results provide a good fit in the HAZ.

3.3. Ballistic testing

The ballistic testing was carried out at the ballistic laboratory at SIMLab. A specially designed smooth-bored Mauser rifle fired 7.62 mm armor piercing (AP) bullets towards the target plates that were mounted in a rigid rack inside a bullet proof impact chamber. The point of impact was adjusted by moving the target, not the rifle. The initial velocity could be predefined with an accuracy of ± 20 m/s by varying the amount of powder in the cartridge. A Phantom v1610 high-speed video camera was, however, used to measure the exact initial (striking) and residual velocities. Figure 8 shows pictures of the perforation process.

A total of nine shots were fired into the 10 mm thick flat aluminum extrusion: four in the base material, four in
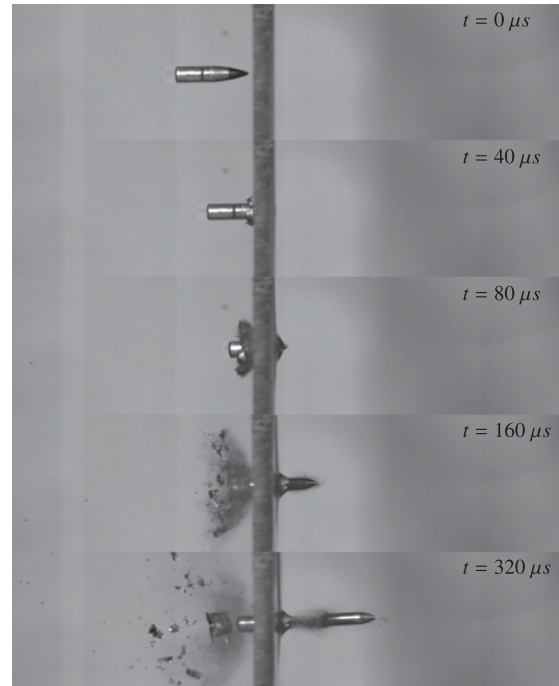
Figure 8. Image sequence showing the perforation process of the 10 mm thick aluminum extrusion.

the HAZ and one in the weld. However, no simulations were done of the weld consumable, so this result is omitted in the following[1]. We did not have enough material to experimentally determine the ballistic limit velocities for the cases mentioned above so they were approximated by curve-fitting Eq. (2) in the same way as for the numerical results. Figure 4 compares the numerically obtained results to the experiments, and the correspondence is in some cases excellent, but generally good.

The material is affected by heat, and is thus weaker than the base material, up to approximately 20 mm from the weld center. This means that potentially a 40 mm wide area exists where the ballistic capacity of the welded component is weakened. Of course the material has a strength gradient in the HAZ which makes is difficult to determine exactly what the strength is at the point of impact in the experiments. Figure 4b shows that the experimental ballistic tests lie within the spread from the numerical simulations which is sensible considering that the experiments were in fact affected by the entire extent of the HAZ.

The numerically predicted ballistic limit velocity for the base material is only 3 m/s higher than the experimentally determined one (347 m/s compared to 344 m/s). In fact, this gives a relative difference of less than 1% which is a remarkable result.

As mentioned, only one ballistic limit velocity was determined experimentally in the HAZ and the value is 312.0 m/s, i.e., 9.3% lower than in the base material. The numerical simulations provided enough data to predict ballistic limit velocities for a range of material behaviors at different distances from the weld center line. The weakest

---

[1] The approximated v_{bl} from the weld is slightly lower than the base material, but significantly higher than the HAZ [7].

material was found 8.1 mm from the weld center line and the strongest was found closest to the base material, i.e., at $x = 14.1$ mm. The averaged simulated ballistic limit velocity from the HAZ was 309.0 m/s which is approximately 1% lower than that of the experiments.

4. Concluding remarks

In this study the perforation resistance of welded aluminum extrusions was successfully predicted based only on numerical simulations.

The base material, as expected, exhibited the highest capacity in both the numerical simulations and the experiments. The material behavior was validated and a tension test was simulated giving excellent correspondence, as shown in Fig. 5. Figure 4a shows that the numerical simulations predicted the ballistic behavior accurately with almost no discrepancy from the experimental result. Of course, many uncertainties exist in the experimental work, and several assumptions have been made in the numerical procedure.

The predominant failure mode in all the experiments was ductile hole-growth, suggesting that the modeling approach as described in Sect. 2 with an initial pin hole in the material is an acceptable approximation.

Figure 4b shows the experimental results at the center of the spread from the numerical simulations. Despite our best aiming-efforts, we can not change that the diameter of the bullet is nearly the same size as the entire extent of the HAZ and only one ballistic limit velocity can be found from the experiments. This result should, in theory, reflect the average behavior of the HAZ – which it does.

To conclude: The numerical results are in good agreement with the experimental data, and the deviation is never more than 10%. We showed that without carrying out a single experiment, we can predict the ballistic behavior of welded Al-Mg-Si aluminum alloy extruded profiles subjected to small-arms bullets with good accuracy. It is believed that the proposed modeling approach can become very useful in preliminary design of aluminum protective structures.

References

[1] J. Johnsen, J.K. Holmen, O.R. Myhr, O.S. Hopperstad, T. Børvik, Computational Materials Science **79**, 724 (2013)

[2] T. Børvik, S. Dey, A.H. Clausen, International Journal of Impact Engineering **36**, 948 (2009)

[3] J.K. Holmen, J. Johnsen, O.R. Myhr, O.S. Hopperstad, T. Børvik, International Journal of Impact Engineering **57**, 119 (2013)

[4] H.G. Fjær, O.R. Myhr, S. Klokkehaug, S. Holm, *Advances in aluminum weld simulations applying WeldSim*, in *Proceedings of the 11th International Conference on Computer Technology in Welding*, edited by T.A. Siewert, C. Pollock (NIST Special Publication, Washington, 2001), pp. 251–263

[5] S.M.W. Breivik, E.F. Thomsen, Master's thesis, SIMLab - Norwegian university of Science and Technology, NTNU (2014)

[6] O.R. Myhr, Ø. Grong, K.P. Pedersen, Metallurgical and Materials Transactions **41A**, 2276 (2010)

[7] J.K. Holmen, T. Børvik, H.G. Fjær, O.R. Myhr, O.S. Hopperstad, Submitted for possible journal publication (2015)

[8] *IMPETUS Afea Solver* (Cited 2014-20-10), http://www.impetus-afea.com

[9] T. Børvik, O.S. Hopperstad, T. Berstad, M. Langseth, European Journal of Mechanics - A/Solids **20**, 685 (2001)

[10] G.R. Johnson, W.H. Cook, *A constitutive model and data for metals subjected to large strains, high strain rates and high temperatures*, in *Proceedings of the 7th International Symposium on Ballistics* (The Hague, Netherlands, 1983), pp. 541–547

[11] M.J. Forrestal, T. Børvik, T.L. Warren, Experimental Mechanics **50**, 1245 (2010)

[12] R.F. Ipson, T.W. Ipson, Journal of Applied Mechanics **30**, 384 (1963)

[13] O.R. Myhr, Ø. Grong, S.J. Andersen, Acta Materialia **49**, 65 (2001)